DOI: 10.61782/fa.2023.0792

forum acusticum 2023

INFLUENCE OF CHORD LENGTH AND LOAD DISTRIBUTION MODIFICATION ON THE SOUND EMISSION AND EFFICIENCY OF A BENCHMARK FAN

Julian Benz[1*] **Felix Czwielong**[1*] **Andreas Renz**[1] **Christof Ocker**[2]
Michael Sedlmajer[2] **Markus Merkel**[2] **Stefan Schoder**[3] **Stefan Becker**[1]
[1] Institute of Fluid Mechanics, Friedrich-Alexander-University Erlangen-Nuremberg, 91058 Erlangen, Germany
[2] Aalen University of Applied Sciences, 73430 Aalen, Germany
[3] Institute of Fundamentals and Theory in Electrical Engineering, TU Graz, 8010 Graz, Austria

ABSTRACT

The design parameters of axial fans, such as load distribution over the blade, chord length and the angle of attack, significantly influence the resulting aerodynamic and aeroacoustic properties of the fans. Based on an international benchmark fan, its design parameters were modified and two additional fans were created. In the process, all three fans had the same specific load, but in one case the chord length of the fan was varied and in the second case an additionally modified load distribution was applied. The modified load distribution is based on Prandtl's idea that a bell-shaped load distribution has the lowest induced drag on aircraft wings by reducing the wing tip vortex. The numerical investigations demonstrated that this reduction can be also achieved on axial fans leading to increased aerodynamic efficiency. By using the Lighthill analogy, a decrease in the sound emission of the fan could be found. In addition, the modification with the increased chord length exhibits improved aerodynamic and acoustic properties compared to the benchmark fan.

Keywords: *axial fan, load distribution, chord length, CFD, CAA*

**Corresponding author*: julian.benz@fau.de, felix.czwielong@fau.de.
Copyright: *©2023 Julian Benz et al. This is an open-access article distributed under the terms of the Creative Commons Attribution 3.0 Unported License, which permits unrestricted use, distribution, and reproduction in any medium, provided the original author and source are credited.*

1. INTRODUCTION

Axial fans have a wide range of applications and they are often used in the direct vicinity of humans. In conjunction with the aim of sustainability an efficient and quiet axial fan is desirable. In the design of axial fans, there are many degrees of freedom, and together with the instationary turbulent flow, there exists a certain complexity. The complexity increases even further when not only the aerodynamics plays a role, but also the acoustics. This is because of the noise generated due to the turbulence and so at first it would be suspected that an aerodynamic optimisation would also result in an improvement of the acoustic properties. But this is generally not the case which was shown for example, by Becker et al. in [1]. However, it is possible to identify different regions of sound sources on axial fans. On axial fans, profiled airfoils are used for the fan blades. According to Blake [2], there are different flow induced sound sources existing on a stationary airfoil in an airflow: 1. Leading edge sound – typically a low frequency broadband sound, 2. Trailing edge sound – a high frequency broadband sound, that arises from the boundary layer flow separation, 3. Local amplitude peaks – created by vortex shedding. Additionally, on a ducted axial fan there are two more sound sources occurring according to Wright [3], which are: 4. Tonal components – from transient pressure fluctuations, 5. Subharmonic narrowband humbs - relative high sound pressure levels which are generated by the vortex system in the tip gap region. In various research projects different possibilities have been investigated on how axial fans can be modi-

fied to improve their aerodynamic and aeroacoustic properties. For example, there is the possibility to add turbulators and flow deflection structures on the surface of the blade [4, 5], serrating or slitting the leading and/or trailing edge [6–9], or using winglets or endplates on the blade tip on the fan [5, 10]. However, all these modifications increase the complexity of the geometry, leading to increased manufacturing difficulty and hence higher production costs. In contrast, changing the load distribution of axial fans does not increase the manufacturing difficulty, because the basic shape of the fan blade won't become more complex. By modifying a specific area of the fan blade where any of the above mentioned sound sources are located, the noise characteristics of a fan can be improved. An area with high improvement potential is the fan blade tip. The reason is that the vortex system in the tip gap region has not only a significant influence on the acoustics, but also a strong impact on the aerodynamic efficiency of the fan. The aerodynamic efficiency of axial fans (η) can be calculated with the volume flow rate ($\dot{V}$), the pressure rise through the fan between the suction and pressure side (Δp), the rotational speed (n) and the torque (M) with Eq. (1).

$$\eta = \frac{\dot{V}\Delta p}{2\pi n M} \tag{1}$$

The formation of the blade tip vortex occurs due to the pressure difference between the upper and lower side of the profile at the tip of the blade. In general, a smaller tip gap distance reduces the flow velocity at the tip gap and also the size of the vorticity in the tip gap area [11]. However, it is not possible to decrease the dimension of the tip gap infinitely because it would be difficult to manufacture the fan and trouble-free operation couldn't be guaranteed because of the risk of collision between the fan blades and the duct wall. In addition to adjusting the load distribution, it is also possible to modify the chord length of the fan blade. This means that for a given load, the angle of attack of the fan blade can be influenced by changing the chord length. This paper investigates the influence of a modified load distribution and a larger chord length applied to a benchmark fan. The physical mechanism of the modified fan blades is analyzed with numerical time-resolved CFD and CAA simulations. For the acoustic comparison, the sound pressure level (L_p) is calculated with the absolute sound pressure p and the reference sound pressure in air with $p_0 = 2 \cdot 10^{-5}$ pa, see (2).

$$L_p = 20 \log(\frac{p}{p_0}) \tag{2}$$

The direct following section will describe the fans investigated in this paper. The second section will show the simulation setup and its validation. Next, the fans will be investigated in terms of their aerodynamic and acoustic properties. The paper then concludes with a summary and outlook.

2. THE INVESTIGATED FANS

The inspiration on the modification of the work load distribution on axial fans originates from aircraft wings. Similar to fan blades, a vortex at the wing tip of aircraft wings arises. This vortex is responsible for the induced drag, which increases at slower flying speeds and higher angle of attacks [12]. In 1933, Ludwig Prandtl recommended a bell-shaped load distribution for an aircraft wing which has the lowest drag for a given wing structure [13]. This was proven by Bowers et al. in 2016 resulting in a reduced wing tip vortex compared to an elliptical-shaped wing load distribution [14]. The bell-shaped load distribution was applied here to the fan called "Prandtl fan". This fan originates from an international intensively investigated benchmark fan which is called here "Benchmark fan" [15–18]. It was used in this investigation as a reference, because the aerodynamic and acoustic properties are well known, so it was possible to validate the simulation model. The Benchmark fans chord length decreases with an increasing radius on the blade while the Prandtl fan has a constant chord length with 110 mm. The difference in chord length between these two fans is 9.1% at the hub and 45.5% at the tip, with the chord length of the Prandtl fan being greater. The Benchmark fan has an isoenergetic load distribution over the whole blade. To achieve a valid comparison on the influence of the load distribution and chord length a third fan was investigated called "ConstChord fan". This third fan has the same constant chord length as the Prandtl fan and the same isoenergetic load distribution as the Benchmark fan. All three fans are designed with the same total load value and the same airfoil is used which has a NACA 4510 shape. The design point for the fans is at a volume flow rate of $\dot{V} = 1.4\ \mathrm{m^3\,s^{-1}}$ and a rotational speed of $n = 1486\ \mathrm{min^{-1}}$. The bell-shaped load distribution has been modified at the hub area. With the original bell-shaped load distribution, the maximum load value is at the hub. However, since the hub area is susceptible to flow separation, the specific load should not be too high and was therefore reduced to a value that roughly corresponds to that of the other fans. To achieve the same total load on the Prandtl fan, the specific load at

the middle of the blade was increased by 48.3% leading to the load distribution as seen in Fig. 1.

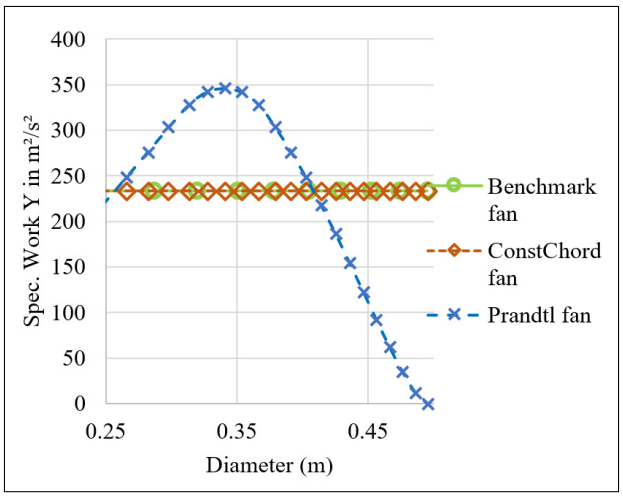

Figure 1: Comparison of the load distribution of the three investigated fans.

3. DESCRIPTION OF THE SIMULATION SETUP

For the numerical simulations, STAR CCM+ (Version 17.02.007) was used. To decrease the computational effort, the simulation was divided into several parts using different turbulence models and different timesteps. At first, for the initialisation of the flow field, a stationary RANS was used. After that, it was switched to a LES with a time step of $t = 10^{-4}$ s to calculate the large, high energy containing eddies in an efficient way. Finally, the time step was reduced to $t = 2.083 \cdot 10^{-5}$ s to compute the smaller eddies. The acoustic data gets recorded after a defined settling time of the small time step over a period of 1.11 s. The basic dimensions of the simulation model are oriented on the test rig of the LSTM in Erlangen [19]. For the spatial discretisation, a parametric grid with polyhedral mesh cells with a relative reference to a base size variable was chosen. While for the surface layer a fixed parametrisation with prism layer cells has been used. The resulting mesh can be seen in Fig. 2. The rotation of the fan was realised with the moving reference frame method. The acoustics were recorded via seven microphones similar to the experimental investigations with the Benchmark fan from [18]. The microphones are positioned on a sub circuit with a radius of $R = 1$ m in front of the duct on the suction side of the fan. In the simulation setup, the microphones are in the 50% refinement region as shown in Fig. 2 and with a base size of 10 mm this leads to a threshold frequency of $f_{max} = 3.81$ kHz for the acoustics with an estimated point per wavelength of PPW = 18. For the computation of the acoustics, the Lighthill analogy was used. The acoustic pressure from the measurements and simulations were energetically averaged over the microphone positions and a linear spectrum was formed using a FFT.

4. VALIDATION OF THE SIMULATION MODEL

The validation of the simulation model was done for the aerodynamic and acoustic properties with the benchmark fan. For the aerodynamic validation, a reference pressure value of an experimental investigation from Junger et al. [18] was used. Besides the base size, the turbulence model, the wall model, the calculation method for the wall and the number of inner iterations were varied. An overview of the variation for the aerodynamic validation is given in Tab. 1. N-WC stands there for the calculation method for the wall called Near-Wall Cell which means that the closest grid cell to the wall is used for the calculation of the boundary layer. O-WC means that the second closest grid cell to the wall is used for the calculation of the boundary layer. The smallest deviation to the reference pressure was achieved with a base size of 8 mm. However, the 8 mm base size resulted in the highest grid cell number of 82.4 mio. cells. For the following simulation, a base size of 10 mm with a wall modeled All-y+ wall treatment LES, O-WC and 5 inner iterations resulting in a cell number of 45.2 mio with a deviation to the reference pressure of 3.4% was chosen. With this setup, the relative reference pressure deviation is comparatively a bit higher by 1.9% to the 8mm base size, but the number of cells is reduced by 45.2%, which significantly reduces the computational effort. For the acoustic validation, a base size of 10 mm was also used. The turbulence models, wall models and calculation methods from the aerodynamic validation were varied for the acoustic validation to investigate their influence on the acoustics. In Fig. 3, the resulting sound pressure spectrum is shown and compared to an additional experimental measurement of the used benchmark fan. Comparing the different spectrums, it can be noticed that the wall models and calculation method for the wall have a relatively small influence on the acoustics. However, the difference from the turbulence model from the DES to the LES is significant. The DES has a higher deviation in terms of the overall sound pres-

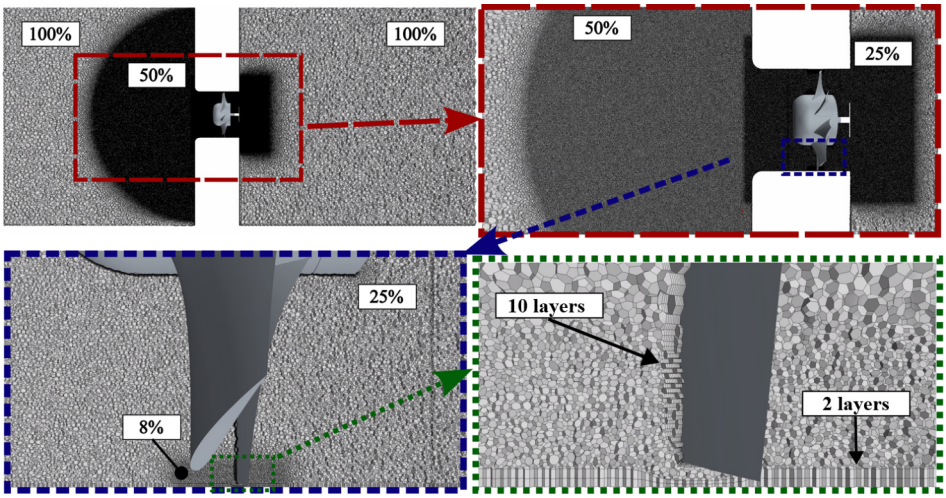

Figure 2: The resulting mesh with the different refinement areas.

sure level and at frequencys $f > 1000$ Hz an increased damping of the sound pressure levels is shown, as with the LES. This could be caused from different resolved turbulent scales in certain areas. The overall sound pressure level deviation compared to the experimental measurement is $\Delta L_p = 1.8$ dB. Comparing the spectrum from the simulations to the experimental measurement with a measuring time of $t = 30$ s, an underestimation of the first blade passing frequency ($f \approx 223$ Hz) and at the first subharmonic and second subharmic hump an overestimation is noticeable. Further investigations showed that the underestimation of the first blade passing frequency occurs because of the used moving reference frame rotation method. However, this method is efficient in terms of the computational effort. The alternative, which is the rigid body motion, results in approximately 10-times higher computational costs and that's why it wasn't chosen for this research. Between $f = 700$ Hz and $f = 3500$ Hz, the simulation shows only minor deviations to the experimental data. Comparing the simulation against 30 seperated measurements with a measuring time of $t = 0.5$ s, which shows the variation of the measuring signal, it can be seen that the deviations of the simulation is acceptable. The cutoff frequency is at $f = 3500$ Hz, which correlates with the predicted one. So the validated setup from the aerodynamic side is also valid on the acoustic side.

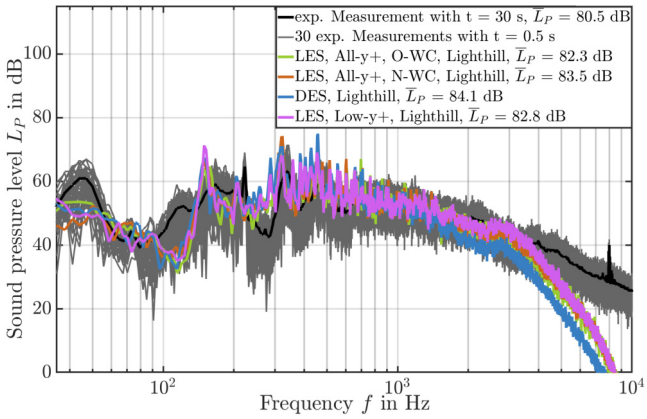

Figure 3: Sound pressure spectra with the overall sound pressure level from different simulation settings and an experimental measurement for the validation.

5. ACOUSTIC INVESTIGATIONS OF THE FANS

Comparing the sound pressure spectra of the three fans in Fig. 4, a reduction at the overall sound pressure level from the Benchmark fan to the Prandtl fan of $\Delta L_p = 3.6$ dB and from the benchmark fan to the ConstChord fan of $\Delta L_p = 5.1$ dB was calculated. Between $f = 15$ Hz and $f = 120$ Hz, the modified fans are up to 5 dB quieter. At $f = 320$ Hz, there is a reduction in the sound pressure level noticeable of up to 10 dB and the broadband noise

Table 1: Variation of the simulation settings with the results for the aerodynamic validation.

Base size in mm	14	12	10	10	10	10	8
Turbulence model	LES	LES	LES	LES	DES	LES	LES
Wall model	All-y+	All-y+	All-y+	All-y+	All-y+	Low-y+	All-y+
Calculation method for the wall	O-WC	O-WC	O-WC	N-WC	-	N-WC	O-WC
Count of the inner iterations	5	5	5	5	5	15	5
Cell number •10⁶	16.86	26.76	45.20	45.20	45.20	61.90	82.40
Pressure difference in Pa	120.36	120.89	122.20	118.76	112.34	119.37	124.60
Rel. Deviation of pressure dif. in %	4.9	4.4	3.4	6.1	11.2	5.6	1.5
Efficiency factor in %	48.65	43.69	45.41	45.00	44.82	46.85	45.03

N-WC: Near-Wall Cell - Closest grid cell to the wall will be used for the calculation of the boundary layer
O-WC: Off-Wall Cell - Second closest grid cell to the wall will be used for the calculation of the boundary layer

emission is reduced compared to the Benchmark fan.

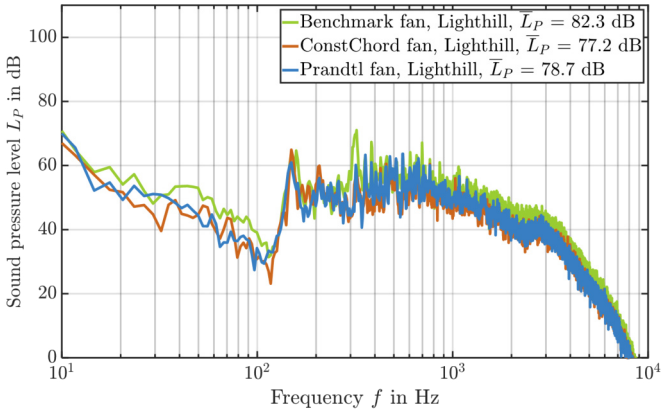

Figure 4: Sound pressure spectra with the overall sound pressure level of the three investigated fans.

The larger chord length has independently of the load distribution positive effects on the acoustics. The difference of the load distributions on the overall sound pressure level is relatively small with $\Delta L_p = 1.5$ dB, which means that the the ConstChord fan is quieter than the Prandtl fan. Analysing the difference between both fans with the spectrum in Fig. 4 is difficult and that's why a 1/24 octave filter was applied to both spectra and then a sound pressure level difference spectrum was created as shown in Fig. 5. Positive values of the sound pressure difference means that the Prandtl fan is quieter. At the first and second subharmonic humb ($f \approx 160Hz$; $f \approx 320Hz$), the Prandtl fan is quieter and this indicates that the vortex system in the tip gap area could be improved. While the broadband noise between $f = 400$ Hz and $f = 3000$ Hz is less for the ConstChord fan.

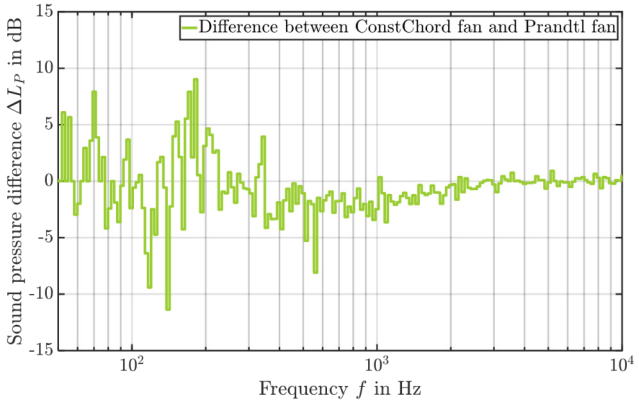

Figure 5: Sound pressure level difference between the ConstChord fan and Prandtl fan spectra by applying a 1/24 octave filter.

Table 2: Aerodynamic characteristic performance datas of the fans.

	Benchmark fan	ConstChord fan	Prandtl fan
Pressure difference in Pa	122.20	122.35	120.90
Effecieny in %	45.41	46.31	47.26
Torque in Nm	2.42	2.33	2.22

6. AERODYNAMIC INVESTIGATIONS OF THE FANS

The better performance of the ConstChord fan in terms of overall sound pressure level cannot be confirmed for the characteristic aerodynamic performance data compared to the Prandtl fan, as shown in Tab. 2. While the ConstChord fan has an increased efficiency of 0.9% compared to the Benchmark fan, the Prandtl fan's efficiency is increased by 1.85%. This better efficiency shows up also in the needed torque to achieve the desired rotational speed. For the Prandtl fan 8.3% less torque is needed, while for the ConstChord fan only a reduction of 3.7% is achieved compared to the Benchmark fan. The findings of Becker et al. [1] are confirmed, that an aerodynamic improvement doesn't mean a clear acoustic improvement at the same time transferred here on axial fans. Analysing the flow field of the fans explains the performance of the fans. By looking at the Q-criteria in Fig. 6-(a)-(d)-(g) it is visible that the larger chord length reduces the vortex creation over the whole blade area and especially in the tip gap region a significant improvement is visible. The bell-shaped load distribution (Fig. 6-(g)) compared to the isoenergetic load distribution (Fig. 6-(d)) with the same chord length even ensures less vortex creation in the tip gap region. This behavior can be explained by looking at the tip gap leakage velocity in Fig. 6-(b)-(e)-(h). The leakage flow on the Prandtl fan starts closer to the trailing edge and the velocity is smaller compared to the ConstChord fan. The reason for the higher broadband sound emission of the Prandtl fan can be found in Fig. 6-(c)-(f)-(i) in which the vorticity between the fan blades is shown. It is shown that the vortex in the wake gets less deflected to the pressure side of the Prandtl fan and this leads to a more turbulent inflow to the downstream fan blade. So the turbulent interaction between the fan blades in the tip gap region with the bell-shaped load distribution is higher compared to the isoenergetic load distribution which leads to the higher broadband sound emission.

7. CONCLUSION AND OUTLOOK

To investigate the influence of the chord length and load distribution on the aerodynamic and acoustic properties of axial fans a simulation model was created. The model was validated with experimental data from a benchmark fan. In the validation a deviation from the reference pressure of 3.4 % and on the acoustic side and a deviation in the total sound pressure level of $\Delta L_p = 1.8$ dB was achieved. It was shown that with a larger chord length a benchmark fan could be aerodynamically and acoustically improved while obtaining the same isoenergetic load distribution on the fan blades. By obtaining the larger chord length and changing the load distribution to a bell-shaped load distribution, further aerodynamic improvement could be achieved. For the acoustics and the bell-shaped load distribution, the sound pressure levels at the second subharmonic humb and at the blade passing frequency were reduced while the broadband sound emission was higher. The source for this higher broadband emission is the general higher turbulent flow interaction between the fan blades because of less deflection of the tip gap vortex to the pressure side. A simulation model was created with which, in a relatively short period of time, the aerodynamic and acoustic properties of a fan can be determined. The investigations will be extended with aerodynamic partial load flow working points in the future. The three analysed fans have already been manufactured with a metal SLM printer and so they will be also investigated experimentally.

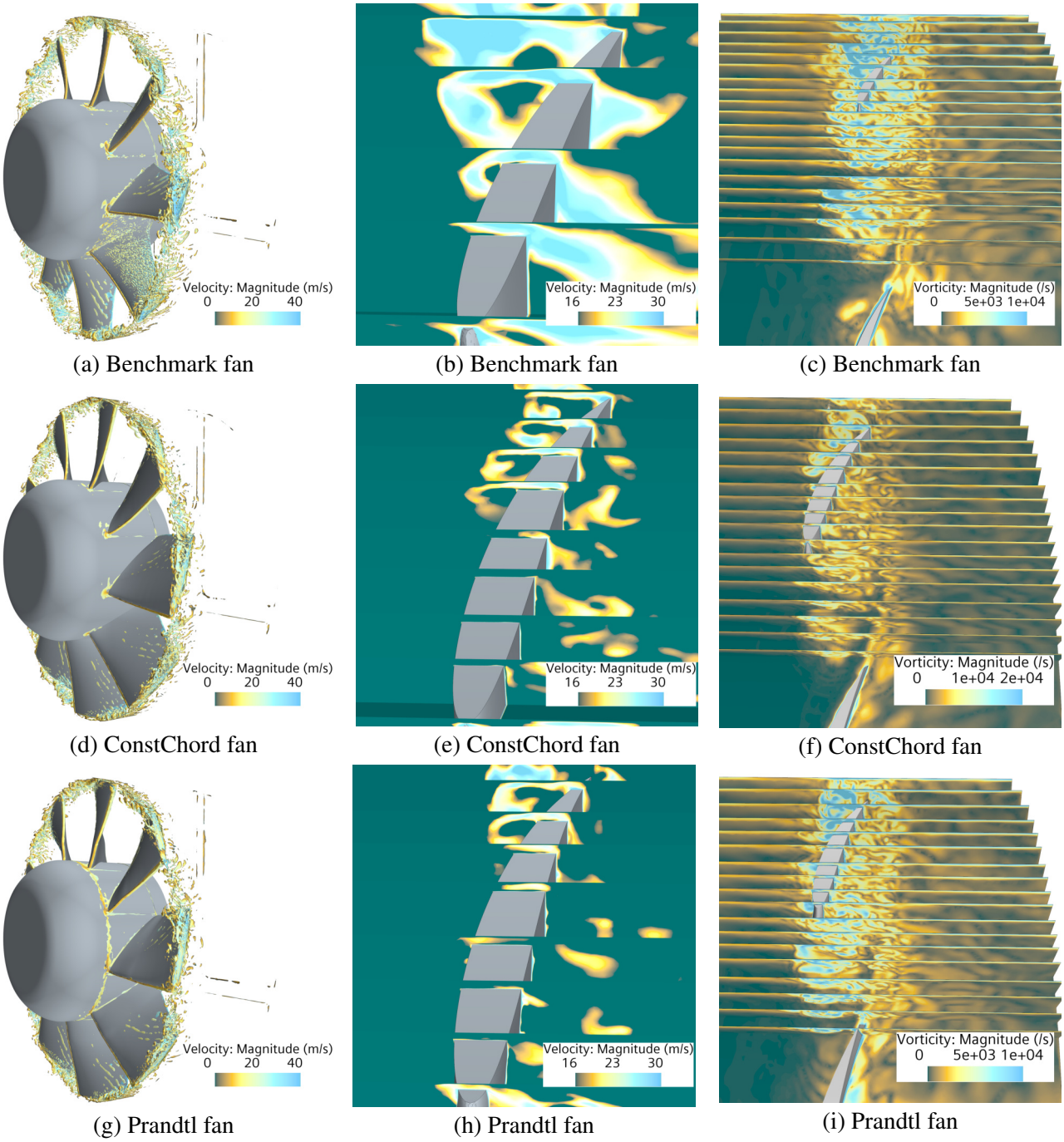

(a) Benchmark fan (b) Benchmark fan (c) Benchmark fan

(d) ConstChord fan (e) ConstChord fan (f) ConstChord fan

(g) Prandtl fan (h) Prandtl fan (i) Prandtl fan

Figure 6: **(a), (d), (g)** Q-Critria und Isosurface with the velocity on it of the fans; **(b), (e), (h)** Tip gap leakage velocity; **(c), (f), (i)** Vorticity between the fan blades.

8. REFERENCES

[1] S. Becker, M. Kaltenbacher, I. Ali, C. Hahn, M. Escobar, A. Kaltenhauser, and F. Ullrich, "Aeroacoustic investigation of the flow around cylinder geometries - a benchmark test case," 2007.

[2] W. K. Blake, *Mechanics of Flow-Induced Sound and Vibration Vol. 2 Complex Flow-Structure Interactions*. Elsevier Science and Technology Books, 2017.

[3] S. Wright, "The acoustic spectrum of axial flow machines," *Journal of Sound and Vibration*, vol. 45, no. 2, pp. 165–223, 1976.

[4] M. Milavec, B. Širok, D. V. de Ventos, and M. Hočevar, "Influence of the shape of the blade tip on the emitted noise in the air-gap between the rotor and the housing of an axial fan," *Forschung im Ingenieurwesen*, vol. 78, no. 3-4, pp. 107–119, 2014.

[5] M. Stadler, M. B. Schmitz, P. Ragg, D. M. Holman, and R. Brionnaud, "Aeroacoustic optimization for axial fans with the lattice-boltzmann method," in *Volume 3: Cycle Innovations Education Electric Power Fans and Blowers Industrial and Cogeneration*, American Society of Mechanical Engineers, 2012.

[6] S. Becker, J. Riedel, M. Kaltenbacher, S. Schoder, and F. Czwielong, "On the fluid mechanical and acoustic mechanisms of serrated leading edges," *TUprints*, 2022.

[7] H. M. Lee, K. M. Lim, and H. P. Lee, "Reduction of ceiling fan noise by serrated trailing edge," *Fluctuation and Noise Letters*, vol. 17, no. 03, p. 1850026, 2018.

[8] V. Singh and N. A. Baraiya, "A review on design and optimisation of axial fan," in *Lecture Notes in Mechanical Engineering*, pp. 191–204, Springer Nature Singapore, 2022.

[9] C. Ocker, F. Czwielong, P. Chaitanya, W. Pannert, and S. Becker, "Aerodynamic and aeroacoustic properties of axial fan blades with slitted leading edges," *Acta Acustica*, vol. 6, p. 48, 2022.

[10] A. Corsini and A. G. Sheard, "End-plate for noise-by-flow control in axial fans," *Periodica Polytechnica Mechanical Engineering*, vol. 57, no. 2, p. 3, 2013.

[11] S. M. A. Moghadam, M. Meinke, and W. Schröder, "Numerical analysis of the acoustic field of a ducted axial fan at varying tip clearances," *Acta Acustica united with Acustica*, vol. 105, no. 1, pp. 43–55, 2019.

[12] H. Oertel, ed., *Prandtl - Fuehrer durch die Stoemungslehre*. Springer Fachmedien Wiesbaden, 2012.

[13] W. Tollmien, H. Schlichting, and H. Görtler, *Ludwig Prandtl Gesammelte Abhandlungen*. Springer Berlin Heidelberg, 1961.

[14] A. H. Bowers, O. J. Murillo, R. Jensen, B. Eslinger, and C. Gelzer, "On wings of the minimum induced drag: Spanload implications for aircraft and birds," *NASA STI*, 2016.

[15] S. Schoder, C. Junger, and M. Kaltenbacher, "Computational aeroacoustics of the EAA benchmark case of an axial fan," *Acta Acustica*, vol. 4, no. 5, p. 22, 2020.

[16] F. J. Kroemer, "Sound emission of low-pressure axial fans under distorted inflow conditions," *FAU Forschungen*, vol. Reihe B: Medizin, p. Technik (20), 2018.

[17] F. Zenger, C. Junger, M. Kaltenbacher, and S. Becker, "A benchmark case for aerodynamics and aeroacoustics of a low pressure axial fan," in *SAE Technical Paper Series*, SAE International, 2016.

[18] C. Junger, A. Reppenhagen, M. Kaltenbacher, and S. Becker, "Numerical simulation of a benchmark case for aerodynamics and aeroacoustics of a low pressure axial fan," in *INTER-NOISE and NOISE-CON Congress and Conference Proceedings*, vol. 253, pp. 5785–5791, Institute of Noise Control Engineering, 2016.

[19] F. Czwielong, J. Soldat, and S. Becker, "On the interactions of the induced flow field of heat exchangers with axial fans," *Experimental Thermal and Fluid Science*, vol. 139, p. 110697, 2022.